International Journal of Current Science, Engineering & Technology ISSN : 2581-4311
Original Research Article | Open Access | AMCT 2017 Malaysia | *Special Issue*

Morphological Analysis of Silica-Nickel Oxide Foam Fabricated by Replication Method

Syazwani BAHAROM[a*], Sufizar AHMAD[b] and Hariati TAIB[c]

Faculty of Mechanical and Manufacturing Engineering, Universiti Tun Hussein Onn Malaysia, 86400 Batu Pahat, Johor, Malaysia.

[a]hd140001@siswa.uthm.edu.my, [b]sufizar@uthm.edu.my, [c]hariati@uthm.edu.my

ABSTRACT. Foam materials are very light, but compared with bulk materials, their strength is quite low because of their random structures. Natural lightweight materials such as bone, is a cellular solid with optimized structure. In this research, silica-nickel oxide (SiO_2-NiO) foams were fabricated by a well-known method which is replication method. The compositions of SiO_2-NiO foams consist of 55 wt.% of silica (SiO_2) powder and 10 wt.% of nickel oxide (NiO) powder. SiO_2 and NiO powders were mixed together with binders; polyethylene glycol (PEG) and carboxymethyl cellulose (CMC) to prepare slurry solution for replication of polyurethane (PU) sponge which functioned as the template. 10 wt.% of SiO_2-NiO foams sintered at different temperatures; 1000 °C, 1100 °C, 1200 °C and 1300 °C. Morphology of 10 wt.% of SiO_2-NiO foams such as the structure of foams and particles distribution were studied by using scanning electron microscopy (SEM).

Keywords: *Slurry method, Catalytic, Gas Conversion, Methane reforming, Reticulated;*

Received: 15.10.2017, Revised: 15.12.2017, Accepted: 30.02.2018, and Online: 20.03.2018;

DOI: ***10.30967/ijcrset.1.S1.2018.396-402***

Selection and/or Peer-review under responsibility of Advanced Materials Characterization Techniques (AMCT 2017), Malaysia.

1. INTRODUCTION

Porous materials show a dramatic development nowadays instead of solid materials in various applications such as catalysis, filtration, thermal insulation and performs for metal-ceramic composites, biomedical implants and high-efficiency combustion burners [1]. The advantages of using porous ceramics in these applications are high melting point, high corrosion, and wear resistance, low thermal mass, low thermal conductivity, controlled permeability, high surface area and low density [2]. In order to produce porous ceramics with controlled microstructure, there are many novel methods have been developed in response to the increasing number of new potential applications for cellular ceramics. The fabrication method chosen will determine the range of porosity, the pore size distribution, and the pore morphology [3]. It is well said that processing route or fabrication method for the production of porous material highly influences the microstructural features.

Several types of materials are identified as common support materials, for example, alumina (Al_2O_3), silica (SiO_2), magnesium oxide (MgO), zirconia oxide (ZrO_2) and olivine ($(Mg, Fe)_2SiO_4$) which have been investigated as catalyst support because the catalytic activity of nickel also influenced by its interaction with support materials [4]. In this study, SiO_2 was used as the support for the catalyst or additive that was nickel oxide (NiO). Majewski et al. [5] stated that SiO_2 has strong structural robustness which is stable even at elevated temperature and chemically inert. It makes SiO_2 attractive as a catalyst support and presents the advantage of mechanical strength and has a strong interaction with metal [5]. Besides that, the advantages of using SiO_2 as the support for NiO particles are because SiO_2 is active for methane reforming and more resistant towards carbon formation [6].

Additives play an important role in defining the rheological behaviour of suspensions and the mechanical properties of green and sintered bodies [7]. Nickel is considered a good replacement for noble metals instead of other noble metal-supported catalysts such as rhodium (Rh), ruthenium (Ru), palladium (Pd), platinum (Pt), iridium (Ir), due to its comparable catalytic performance and low cost [6,8].

2. MATERIALS AND METHODS

Silica (SiO_2) and nickel oxide (NiO) are two main raw materials in SiO_2-NiO foam fabrication. Replication method is used to fabricate SiO_2-NiO foam by using polyurethane (PU) sponge as template and it has been cut in cylindrical shape with dimension 26 mm height and 13 mm diameter. To fabricate SiO_2-NiO foam, 55 wt.% of SiO_2 and 10 wt.% of NiO were poured into distilled water and mixed with binders. The binders used in this method were 2.5 wt.% of polyethylene glycol (PEG) and 2.5 wt.% of carboxymethyl cellulose (CMC). The mixture of raw materials, binders and distilled water produced slurry solution for impregnation of PU sponge as a template in making porous material. The impregnated sponge was left for drying in oven for 24 hours at 80 °C before sintered at 1000 °C, 1100 °C, 1200 °C and 1300 °C with 2 °C/min heating and cooling rate in programmable furnace.

The morphological analysis for SiO_2-NiO foam was carried out by using scanning electron microscopy (SEM) and electron dispersive X-ray spectroscopy (EDS).

3. RESULTS AND DISCUSSION

The morphology of SiO_2-NiO foam with 10 wt.% of NiO composition was observed using SEM at different sintering temperatures of 1000 °C, 1100 °C, 1200 °C and 1300 °C as shown in Fig. 1 (a-d). From observation, SiO_2-NiO foams with 10 wt.% of NiO composition sintered at different sintering temperatures also consisted of open pore, close pore and interconnected window cells by struts. The open pore size of SiO_2-NiO foams observed was in the range of 130 µm up to 537 µm.

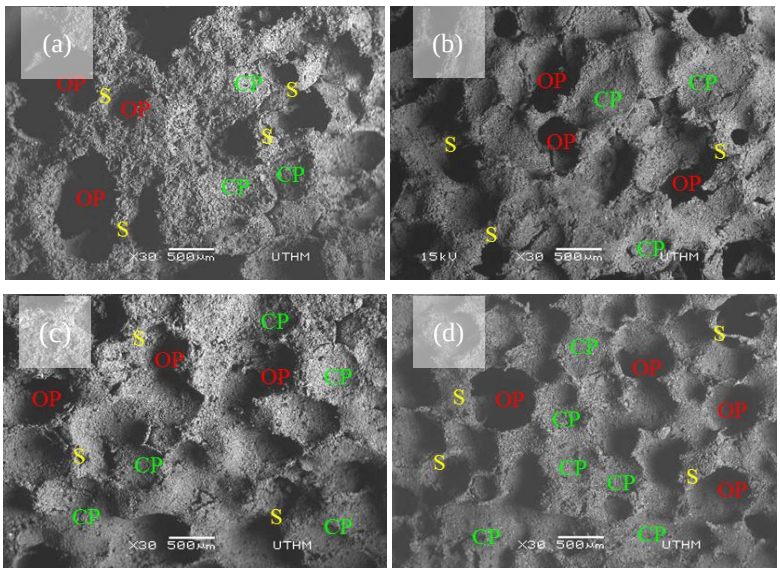

Fig. 1 Morphology of the silica-nickel oxide foam sintered at (a) 1000 °C, (b)1100 °C, (c)1200 °C and (d)1300 °C. (OP=Open pore, CP=Close pore, S=Strut)

Sintering temperature also affect the morphology of the foam as shown in the micrographs in Fig. 1 as the open pore distribution on SiO_2-NiO foam sintered decreased and the pore size became smaller as the

sintering temperature increased. Open pore distribution on SiO_2-NiO foams sintered decreased and the pore size became smaller as the sintering temperatures increased. This is due to the shrinkage and densification of the samples as the sintering temperature increased. The presence of closed cells on SiO_2-NiO foam sintered at 1200 °C and 1300 °C became dominant as marked in micrographs compared to SiO_2-NiO foam sintered at 1000 °C and 1100 °C. The decreasing of open cell window could be explained by the increasing difficulty for ceramic slick removal at higher solid loading during manufacturing, leading not only to a higher density, but also to a higher number of close pores, and strongly influencing the permeability of the foams [9].

Both of SiO_2-NiO foams sintered at 1200 °C and 1300 °C showed increasing size of struts as the NiO compositions and sintering temperatures increased. The strut size of SiO_2-NiO foams observed at 1200 °C was in the range 80 µm to 330 µm while the strut size of SiO_2-NiO foam at 1300 °C was in the range of 100 µm to 360 µm. Views from previous researchers, the pore size of porous foam for steam methane reforming was uncommon between researcher within the range 0.1 µm to 21 mm [5,10,11]. The open pore size observed of SiO_2-NiO foams was within the range and compatible to be used in steam methane reforming application.

Densification of SiO_2-NiO foams was observed as shown in Fig. 2 (a-d) at different sintering temperatures; 1000 °C, 1100 °C, 1200 °C and 1300 °C. The micrographs in Fig. 2 represented the morphology of SiO_2-NiO foam with 10 wt.% of NiO after sintered at different sintering temperatures. The morphology of SiO_2-NiO foams showed open pore distribution with micro meter size. White spot or powder-like in Fig. 2 (a-d) represented the distribution of NiO particles at different temperatures while the grey structure was the structure of SiO_2. The structure of SiO_2-NiO foams became denser as the sintering temperatures increased from 1000 °C to 1300 °C

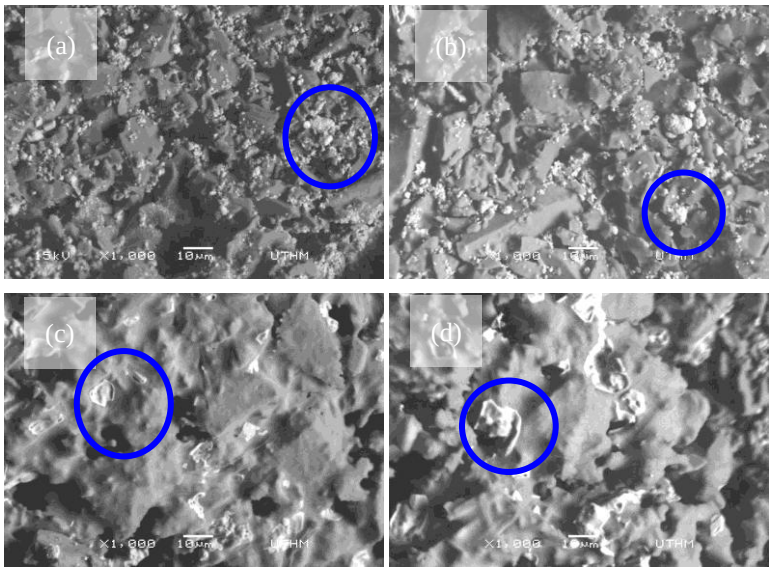

Fig. 2 Morphology of silica-nickel oxide foams at (a) 1000 °C, (b) 1100 °C, (c) 1200 °C, and (d) 1300 °C (= NiO distribution)

Nickel oxide particles distribution were marked by yellow circle while SiO_2 particles distribution was the grey structure where NiO particles distributed on as shown in Fig. 2 (a-d). The distribution of NiO and SiO_2 particles were distinguished by elemental mapping as discussed at Fig. 3. As shown in Fig. 2 (a,b), the particles were initially packed loosely and started to approach and contact to each other as the sintering temperature increased. The growth of grain structure was observed under SEM as the SiO_2 particles and NiO particles started to bond with each other at higher sintering temperature in which denser grain structure was clearly seen at 1200 °C and 1300 °C.

Based on Fig. 2 (a-d), open pore distribution with irregular shape was observed with micro meter size within the range 3 μm up to 20 μm for SiO_2-NiO foams with 10 wt.% of NiO composition. Grano et al. [12] reported that, sintering of nickel crystallite at elevated temperature disrupted the mesoporous SiO_2 template that contributed to the irregular shape on the foam microstructure. The distribution of open pore observed on the surface of SiO_2-NiO foams decreased as the sintering temperature increased due to the increasing in grain size as seen in Fig. 2 (a-d). The larger grains were found to grow and densified, whilst smaller grains and pores that had been created at a lower temperature to accommodate the volume shrinkage associated with reduction were observed to disappear [13].

Elemental mapping was extremely useful for displaying element distributions in textural context, particularly for showing compositional zonation instead of figured out element and mass content. The elemental mapping result showed the particles distribution of elements which existed in SiO_2-NiO foams. The result of elements mapped for 10 wt.% of SiO_2-NiO foams was showed in Fig. 3 (a-d). There was nickel (Ni), silica (Si) and oxygen (O) distributions observed through elemental mapping analysis. The highest distribution of NiO particles was observed at 10 wt.% of NiO composition. This might be due to the excess NiO particles which cannot be mixed with the SiO_2 particles [14]. Fig. 3 shows the elemental mapping test for SiO_2-NiO foam using Electron Dispersive X-ray Spectroscopy (EDS).

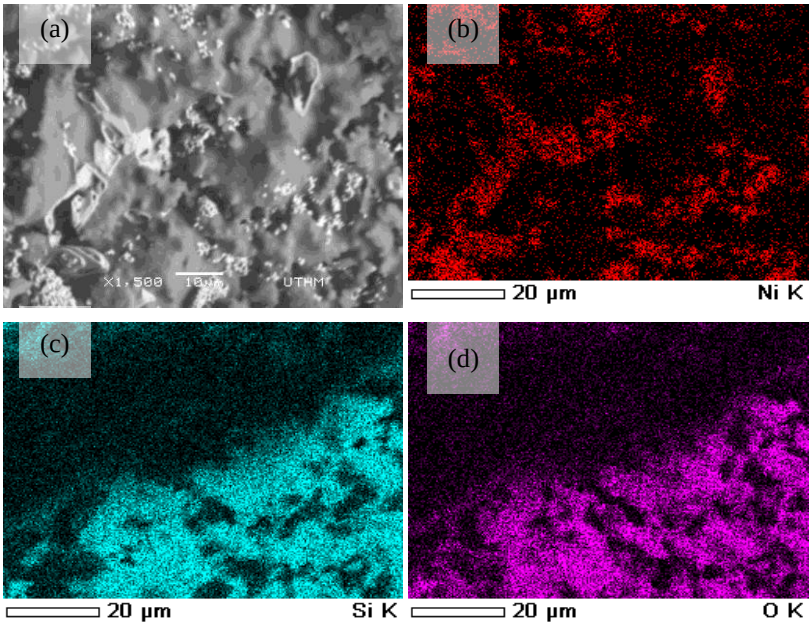

Fig. 3 Element distribution by elemental mapping for 10 wt.% of nickel oxide composition sintered at 1300 °C

Element and phase map were collected automatically and simultaneously. This helped to observe how each element was distributed individually. Fig. 3 (a) was the original image of 10 wt.% of SiO_2-NiO foams. The distribution of Ni, Si and O were differentiated by red, blue and purple colour, respectively in Fig. 3 (b-d). Through the elemental mapping analysis, the white spot as marked in Fig. 2 (a-d) were clarified as Ni particles and the rest of dense structure were Si and O. The colour-image represented the distribution and increased the possibility distinguish the different elements. The distribution of Ni particles was the highest for SiO_2-NiO foams with 10 wt.% of NiO sintered at 1300 °C as proven by EDS result tabulated in Table 1. The purpose to carry out the elemental mapping analysis in this research study was to identify the element and

mass content that existed in SiO_2-NiO foams. A micrograph of 10 wt.% of SiO_2-NiO foams morphology was captured to determine the element and mass content.

The result tabulated in Table 1 showed the mass of different elements such as 20.49% of nickel (Ni), 17.82% of silica (Si) and 17.82% of oxygen (O). The differences in element mass affected the particle distribution. The highest mass of Ni represented the higher distribution of Ni particles on the SiO_2-NiO foams as shown in Fig. 4. This was because the distribution of particles on SiO_2-NiO foams was affected by the early composition of raw material during sample preparation. As the NiO sintering temperature increased, the Ni particles distribution after sintering observed by elemental mapping analysis was increased.

Table 1 Element obtained for 10 wt.% of nickel oxide composition sintered at 1300 °C

Element	Mass (%)
Ni K	61.69
Si K	20.49
O K	17.82
Total	100.00

Fig. 4 (a-d) showed the Ni particles distribution at different sintering temperatures at 1000 °C, 1100 °C, 1200 °C and 1300 °C, respectively.

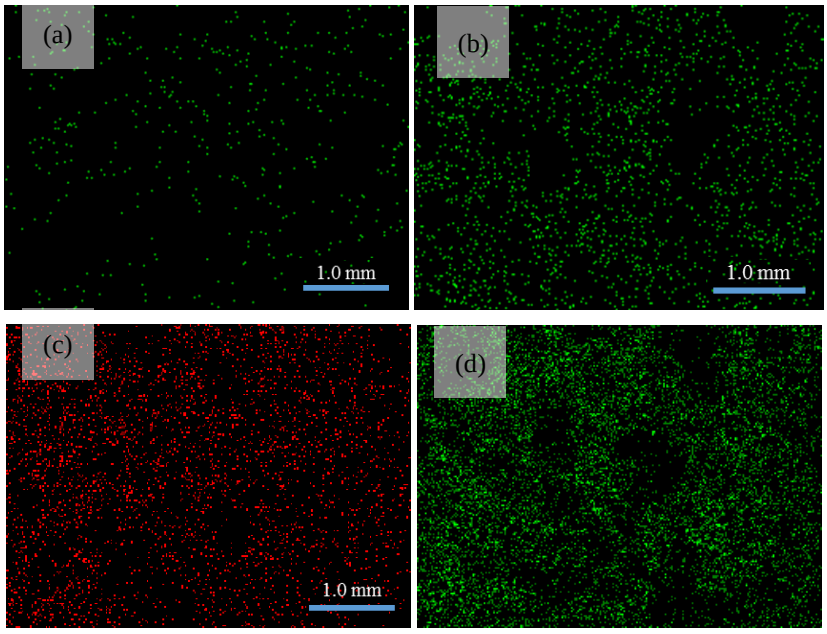

Fig. 4 The distribution of nickel particles of 10 wt.% of silica-nickel oxide foams after sintered at (a) 1000 °C, (b) 1100 °C, (c) 1200 °C and (d) 1300 °C

The distribution of Ni particles increased as the sintering temperatures increased as observed in Fig. 4 (a-d). The lowest Ni particles distribution of SiO_2-NiO foams was observed at temperature of 1000 °C. Lowest distribution observed at lowest sintering temperature due to presence of open pore with macro size and thin strut. At 1300 °C, the highest Ni particles distribution was observed due to the decrease in pore distribution and size, presence a number of close cells and bigger struts. The highest Ni particles indicated the domains contained higher NiO contents than the matrix, which attributed to the formation of NiO-enriched

agglomerates. As sintering temperature increased, the particles gain more energy and collision rate increases [15].

Sintering effect was clearly visible in the SiO_2-NiO foams of the sintered at 1200 °C and 1300 °C as higher Ni particles distribution observed on SiO_2-NiO foams compared to the SiO_2-NiO foams sintered at 1000 °C and 1100 °C. Nickel particles distribution on the surface of SiO_2-NiO foams depended on the structure of SiO_2-NiO foams. Low number of open pore with the larger strut gave Ni particles to distribute more on SiO_2-NiO foams surface. Larger strut with denser structure associated with the grain growth as the sintering temperatures increased. The structure of materials sintered at high temperatures indicated signs of particle grain growth and also substantiated by the grain size distributions [16].

4. SUMMARY

The morphology of 10 wt.% of SiO_2-NiO foams was affected by the compositions and sintering temperatures. Both of them affected the open pore size and distribution, closed pore and strut size

which connected the cell windows together. The open pore size and distribution decreased as the compositions and sintering temperature increased. The number of closed pore became dominant at high temperatures. The size of struts also bigger as densification occurred as sintering temperature increased. Thus, the highest of Ni particles distribution was observed at the highest sintering temperature which was 1300 °C.

REFERENCES

[1] E. Hammel, O. Ighodaro, O. Okoli, In situ-growth of silica nanowires in ceramic carbon composites, Ceram. Int., 40 (2014) 15351-15370.

[2] A. Studart, U. Gonzenbach, E. Tervoort, L. Gauckler, Materials from foams and emulsions stabilizes by colloidal particles, J. Am. Ceram. Soc., 89 (2006) 1771-1789.

[3] F.A.C. Oliveira, S. Dias, M. Vaz, J. Fernandes, Behaviour of open-cell cordierite foams under compression, J. Eur. Ceram. Soc., 26 (2006) 179-186.

[4] R. Widyaningrum, T. Church, M. Zhao, A. Harris, Mesocellular foam silica-supported Ni catalyst to enhance H_2 production from cellulose pyrolysis, Int. J. Hydrogen Energy., 37 (2012) 9590-9601.

[5] A.J. Majewski, J. Wood, W. Bujalski, Nickel-silica core@shell catalyst for methane reforming, Int. J. Hydrogen Energy, 38 (2013) 14531-14541.

[6] H. Wu, V.L. Parola, G. Pantaleo, F. Puleo, A.M. Venezia, F. Liotta, Ni-based catalysts for low temperature methane steam reforming: recent results on ni-au and comparison with other bi-metallic systems, Catalyst, 3 (2013) 563-583.

[7] S. Gomez, O. Alvarez, J. Escobar, J. Neto, C. Rambo, D. Hotza, Relationship between rheological behaviour and final structure of Al_2O_3 and YSZ foams produced by replica, Adv. Mater. Sci. Eng., 1 (2012) 1-9.

[8] W. Cai, L. Ye, L. Zhang, Y. Ren, B. Yue, X. Chen, H. He, Highly dispersed nickel-containing mesoporous silica with superior stability in carbon dioxide reforming of methane: The effect of anchoring, Ind. Eng. Chem. Res., 7 (2014) 2340-2355.

[9] G.I. Garrido, F.C. Patcas, S. Lang, B. Kraushaar, Mass transfer and pressure drop in ceramic foams: a description for different pore sizes and porosities, Chem. Eng. Sci., 63 (2008) 5202-5217.

[10] S.Z. Abbad, V. Dupont, T. Mahmud, Kinetics study and modelling of steam methane reforming process over a NiO/Al_2O_3 catalyst in an adiabatic packed bed reactor, Int. J. Hydrogen Energy, 42 (2016) 1-5.

[11] E. Franzyck, A. Golebiowski, T. Borowiecki, P. Kowalik, W. Wrobel, Influence of steam reforming catalyst geometry on the performance of tubular reformer-simulation calculations, Chem. Process. Eng., 36 (2015) 239-250.

[12] A. Grano, F. Sayler, J. Smatt, M. Bakker, Alternative etching methods to expand nanocasting, and use in the synthesis of hierarchically porous nickel oxide, zinc oxide, and copper monoliths, J. Mater. Res., 111 (2013) 154-157.

[13] Q. Jeangros, W. Hansen, J. Wagner, C. Damsgaard, Reduction of nickel oxide particles by hydrogen studied in an environmental TEM, J. Mater. Sci., 48 (2013) 2893-2907.

[14] F. Tang, H. Fudouzi, T. Uchikoshi, Y. Sakka, Fabrication of porous ceramics with controlled pore size by colloidal processing, J. Eur. Ceram. Soc., 24 (2004) 341-344.

[15] A. Yakubu, Z. Abbas, M. Hashim, Effect of sintering temperature on $Co_{0.5}Zn_{0.5}Fe_2O_4$ nano-particles evolution and particle size distribution, Adv. Nano., 4 (2015) 37-44.

[16] P. Bhattacharjee, S. Sinha, A. Upadhyaya, Effect of sintering temperature on grain boundary character distribution in pure nickel, Scripta. Mater., 56 (2007) 13-16.